

Nanoparticle BAF312@CaP-NP Overcomes Sphingosine-1-Phosphate Receptor-1-Mediated Chemoresistance Through Inhibiting S1PR1/P-STAT3 Axis in Ovarian Carcinoma

This article was published in the following Dove Press journal:
International Journal of Nanomedicine

Ke Gong¹
Yang Dong¹
Liting Wang¹
Yi Duan²
Jian Yu¹
Ying Sun¹
Min Bai³
Yourong Duan¹ 

¹State Key Laboratory of Oncogenes and Related Genes, Shanghai Cancer Institute, Renji Hospital, School of Medicine, Shanghai Jiao Tong University, Shanghai 200032, People's Republic of China;

²Department of Clinical Medicine, North Sichuan Medical College, Sichuan 637100, People's Republic of China; ³Department of Ultrasound, Shanghai General Hospital, Shanghai Jiao Tong University School of Medicine, Shanghai 200080, People's Republic of China

Correspondence: Yourong Duan
State Key Laboratory of Oncogenes and Related Genes Shanghai Cancer Institute, Renji Hospital School of Medicine, Shanghai Jiao Tong University, 2200/25 Xietu Road, Shanghai 200032, People's Republic of China
Tel/Fax +86-021-64437139
Email yrduan@shsci.org

Min Bai
Department of Ultrasound, Shanghai General Hospital, Shanghai Jiao Tong University School of Medicine, 100 Haining Road, Shanghai 200080, People's Republic of China
Tel/Fax +86-13917045725
Email baimin101@126.com

Purpose: Platinum/paclitaxel-based chemotherapy is the strategy for ovarian cancer, but chemoresistance, inherent or acquired, occurs and hinders therapy. Therefore, further understanding of the mechanisms of drug resistance and adoption of novel therapeutic strategies are urgently needed.

Methods: In this study, we report that sphingosine-1-phosphate receptor-1 (S1PR1)-mediated chemoresistance for ovarian cancer. Then we developed nanoparticles with a hydrophilic PEG2000 chain and a hydrophobic DSPE and biodegradable CaP (calcium ions and phosphate ions) shell with pH sensitivity as a delivery system (CaP-NPs) to carry BAF312, a selective antagonist of S1PR1 (BAF312@CaP-NPs), to overcome the cisplatin (DDP) resistance of the ovarian cancer cell line SKOV3DR.

Results: We found that S1PR1 affected acquired chemoresistance in ovarian cancer by increasing the phosphorylated-signal transduction and activators of transcription 3 (P-STAT3) level. The mean size and zeta potential of BAF312@CaP-NPs were 116 ± 4.341 nm and -9.67 ± 0.935 mV, respectively. The incorporation efficiency for BAF312 in the CaP-NPs was 76.1%. The small size of the nanoparticles elevated their enrichment in the tumor, and the degradable CaP shell with smart pH sensitivity of the BAF312@CaP-NPs ensured the release of BAF312 in the acidic tumor niche. BAF312@CaP-NPs caused substantial cytotoxicity in DDP-resistant ovarian cancer cells by downregulating S1PR1 and P-STAT3 levels.

Conclusion: We found that BAF312@CaP-NPs act as an effective and selective delivery system for overcoming S1PR1-mediated chemoresistance in ovarian carcinoma by inhibiting S1PR1 and P-STAT3.

Keywords: cisplatin, chemotherapy, antagonist of S1PR1, pH sensitivity, nanoparticles

Introduction

Ovarian cancer patients have no obvious symptoms at an early stage, which leads to diagnosis at an advanced or metastatic stage, at which point doctors mainly adopt standard surgery and platinum/paclitaxel-based chemotherapy.¹⁻³ However, chemoresistance occurs due to inherent or acquired resistance, resulting in unsatisfactory results in ovarian cancer.⁴ Ovarian carcinoma is the most common cause of death in women due to its eventual resistance to chemotherapy.⁵ Thus, there is an urgent need to elucidate the underlying mechanisms of drug resistance and find novel potential therapeutic targets to overcome ovarian cancer.

Platinum is a standard treatment for patients with ovarian cancer, and patients receiving platinum therapies tend to upregulate signal transduction and activators of transcription 3 (STAT3) activity.⁶⁻⁸ In addition, by analyzing the original The Cancer Genome Atlas (TCGA) ovarian cancer data, researchers found that Phosphorylated-signal transduction and activators of transcription 3 (P-STAT3) levels were increased in patients who had short survival compared with those in patients with longer survival.⁹ Previous studies have demonstrated that persistent activation of STAT3 leads to uncontrollable tumor proliferation as well as drug resistance in ovarian cancer.^{10,11} However, there seems to be intractable direct suppression of STAT3 activation in the clinic. STAT3 can be activated by multiple chemokines and cytokines;¹² thus, blocking one pathway seems to be insufficient to effectively reverse P-STAT3-mediated drug resistance. A recent study demonstrated that STAT3-induced sphingosine-1-phosphate receptor-1 (S1PR1), a G protein-coupled receptor for sphingosine-1-phosphate (S1P), is crucial for persistent STAT3 activation in tumors,¹³⁻¹⁵ which suggests that targeting S1PR1 can be an effective way to downregulate the activation of STAT3.

The sphingosine analogue BAF312 is a second-generation S1P receptor modulator approved by the United States Food and Drug Administration (FDA) for the treatment of relapsing multiple sclerosis.¹⁶ BAF312, as an analog of S1P and a ligand of S1PR1, competitively and selectively binds to S1PR1, thereby promoting the internalization and degradation of S1PR1.^{17,18} Previous studies have shown that S1PR1 degradation inhibits STAT3 activation and enhances the apoptosis of ovarian cancer cells.¹⁹ Studies have demonstrated that BAF312 (1 h at 1 μ M) promotes significant internalization of the 91% of S1P1 receptors and downregulates S1PR1 expression.²⁰ In addition, a previous study found that fingolimod (FTY720), the first-generation S1PR modulator, can resensitize chemoresistant ovarian cancer cells to cisplatin by downregulating S1PR1.²¹ The efficacy of BAF312 in reversing platinum-resistant ovarian cancer has not yet been evaluated in ovarian cancer.

BAF312 is lipophilic, in order to prolong the blood retention time of the drug, reduce systemic toxicity and side effects in patients and increase the targeting of ovarian carcinoma and the enrichment degree at the tumor site, here, we used nanotechnology to develop DSPE-PEG2000-COOH-CaP (CaP-NPs) incorporating BAF312 as a delivery system to enhance therapeutic efficacy in chemoresistant ovarian cancer. CaP-NPs are considered a biocompatible carrier

with added stability from PEG2000 and were approved by the FDA for use in humans;²² DSPE is the main component of cell membranes, and calcium phosphate (CaP) is an essential element for humans. BAF312-DSPE-PEG2000-COOH-CaP nanoparticles (BAF312@CaP-NPs) are synthesized via a repeatable biomineralization method in which hydrophobic DSPE encapsulating BAF312 forms the compact inner core and hydrophilic PEG2000 with calcium phosphate (CaP) forms the outer shell. BAF312@CaP-NPs have four main advantages: 1. PEG2000 facilitates the long-term circulation of nanoparticles in the human body;²³ 2. A particle size of 120 nm is conducive to enrichment in tumor sites through the EPR effect;²⁴ 3. The negative charge of the nanoparticles and their zeta potential of -10 mV help their long-term circulation, and the particles become positively charged in the acidic niche of the tumor, enabling them to be absorbed by tumor cells, as tumors tend to uptake positively charged particles;^{25,26} 4. The calcium-phosphorus system is pH sensitive, which ensures the release of nanoparticles in the acidic tumor niche.

In sum, our work shows that S1PR1 overexpression affects acquired resistance to chemotherapies in ovarian carcinoma by upregulating P-STAT3. Downregulating S1PR1 with BAF312 could be an effective method, and encapsulating BAF312 with nanotechnology can greatly improve strategies to overcome chemical resistance in ovarian cancer. Our work demonstrates that BAF312@CaP-NPs overcome chemoresistance by inhibiting S1PR1 and P-STAT3.

Materials and Methods

Cell Culture and Treatment

The human ovarian cancer cell line SKOV3 was purchased from the Shanghai Institute of Cell Biology at the China Academy of Sciences. Cells were cultured in DMEM supplemented with 10% fetal bovine serum and 1x penicillin-streptomycin at 37°C in a humidified 5% CO₂ atmosphere.

Preparation of BAF312@CaP-NPs

1,2-Distearoyl-sn-glycero-3-phosphoethanolamine-N-[carboxy(polyethylene glycol)-2000] (DSPE-PEG2000-COOH) was purchased from Ponsure Biotechnology (Shanghai, China). Calcium chloride (CaCl₂) and trisodium phosphate (Na₃PO₄) were purchased from Sigma-Aldrich (USA). BAF312 was purchased from Selleck (Shanghai, China). BAF312-loaded DSPE-PEG2000 micelles were made through thin-membrane hydration. Then, CaCl₂ solution was added to the prepared micelle solution. Finally, HBS (Hepes, Na₃PO₄,

and NaCl; pH 7.4) buffer solution was added into the BAF312-DSPE-PEG2000-Ca²⁺ solution quickly and allowed to incubate at room temperature for 30 min to form BAF312@CaP-NPs. The final concentration of BAF312 was 0.25 μ M. To meet the demands of subsequent experiments, during the preparation of NPs, BAF312 was replaced by rhodamine B (Rb) (Beyotime, China) to prepare Rb@CaP-NPs.

Physical and Chemical Properties of BAF312@CaP-NPs

The Zetasizer IV analyzer (Malvern Zetasizer Nano ZS90, Malvern, UK) was used to evaluate the size and surface potential of BAF312@CaP-NPs. A Talos F200X transmission electron microscope (TEM) was used to confirm the morphology of BAF312@CaP-NPs. The encapsulation efficiency (EE%) and drug loading (DL%) of BAF312 in BAF312@CaP-NPs were determined by high-performance liquid chromatography (HPLC) (Agilent 1100, USA).

In vitro Release of BAF312 from BAF312@CaP-NPs

The release profiles of BAF312@CaP-NPs in vitro were measured using the dialysis assay. A solution containing BAF312@CaP-NPs was dialyzed against PBS buffer solution containing 10 M sodium salicylate at two different pH values (6.0 and 7.4).

Establishment of Drug-Resistant Cells

SKOV3 cells were treated with cisplatin (Sigma-Aldrich, USA) at concentrations ranging from 5 μ M to 30 μ M for up to 2 months; the resulting drug-resistant cells were named SKOV3DR cells. In addition, the parental cells were named SKOV3DP cells.

siRNA Transfection

siRNAs were incubated with cells and Lipofectamine 2000 in 6-well plates when the cells reached 70–80% confluence. Two siRNAs were synthesized by Ribo-Bio (Guangzhou, China). The siRNA sequences were as follows:

negative control siRNA (siNC), ACGUGACACGUUC GGAGAATT; S1PR1-siRNA1, CGCCTCTCCTGCTAA TCA; and S1PR1-siRNA2, CGGTCTCTGACTACGTCAA.

In vitro Cytotoxicity Assay

Cells were collected in the logarithmic growth phase and seeded in 96-well plates at a density of 5000 cells per well.

After they adhered to the plates overnight, the cells were treated with the indicated drugs at certain concentrations for 72 h. 3-(4,5-Dimethylthiazol-2-yl)-2,5-diphenyltetrazolium bromide (MTT) (Sigma, USA) was added to each well, and the cells were incubated at 37°C for 4 h. Then, the liquid was discarded, and Dimethyl sulfoxide (DMSO) (Sigma, USA) was added. The optical densities (ODs) were measured at a wavelength of 492 nm with a microplate reader (Thermo Multiskan FC, USA).

Apoptosis Assay

Cells were seeded in 6-well plates at a density of 5×10^5 cells per well overnight and treated with the indicated concentrations of the indicated drugs for 48 h. Cells were collected and detected by an Annexin V-PE apoptosis detection kit (Vazyme, China). Then, the cells were analyzed by flow cytometer (Becton Dickinson, Franklin Lakes, USA). Analysis of the results was carried out with FlowJo 6.0. Each assay was performed in triplicate.

Calcium and PI Dye Assays

Cells were seeded in 12-well plates at a density of 1×10^5 cells per well overnight, followed by incubation with the indicated drugs for 72 h. After washing with PBS three times, cells were stained with 1 mL 2.0 μ M PI (Beyotime, China) and 2.0 μ M calcium indicator (Beyotime, China) for 30 min, discarded and imaged (Olympus Corporation, Japan).

RNA Isolation and Semiquantitative RT-PCR

Relative mRNA expression in cells after treatment was determined by real-time quantitative RT-qPCR with 10 ng of RNA that was isolated from treated cells using a Total RNA Extract kit (Takara, Japan). cDNA was generated using a Reverse Transcription System kit (Takara, Japan). qRT-PCRs were performed using SYBR Green PCR Master Mix (Takara, Japan). The sequences of the primers used were as follows:

S1PR1, 5'- GCCTCTTCCTGCTAATCAGCG-3' (forward) and 5'- GCAGTACAGAATGACGATGGAG-3' (reverse); and

GAPDH, 5'- ATCAATGGAAATCCCATCACCA-3' (forward) and

5'- GACTCCACGACGTACTCAGCG-3' (reverse);

Relative expression values were normalized to the control value to obtain percent fold changes, and each assay was performed in triplicate.

Western Blot Assay

Whole cells were collected after treatment with the indicated drugs for 48 h, and RIPA lysis buffer containing the protease inhibitor PMSF (Beyotime, China) and a phosphatase inhibitor cocktail (Beyotime, China) was added. The protein samples were separated on a 12% acrylamide gel and then transferred to PVDF membranes. After blocking with 10% (w/v) nonfat milk in TBS containing 0.1% (v/v) Tween 20, the PVDF membranes were incubated with certain primary antibodies at 4°C overnight and then incubated with horseradish peroxidase-conjugated secondary antibodies (Proteintech, USA). Mouse polyclonal antibodies against S1PR1, P-STAT3, and GAPDH were obtained from Santa Cruz Biotechnology (USA). Rabbit polyclonal antibodies against MRP1 and survivin were obtained from Cell Signaling Technology (USA).

Cellular Uptake Assay

Cells were collected and seeded onto coverslips at a density of 5×10^5 cells and allowed to adhere overnight, and then 20 μ L of 1 mg/mL free Rb (Beyotime, China) and Rb@CaP-NPs were added and incubated for 1 h and 4 h. The cells were fixed with 4% (w/v) paraformaldehyde for 15 min, washed with PBS twice and counterstained with DAPI (Beyotime, China). Slides were mounted, and images were captured using a Zeiss LSM510 Meta inverted confocal microscope (Germany).

TCGA Data Analysis

S1PR1 expression and the related data in patients with ovarian cancer from the TCGA portal (<https://cancergenome.nih.gov/>) were downloaded and analyzed. Information on the ovarian cancer patients included survival times. The selected ovarian cancer patients were assigned into two groups according to patient overall survival (OS). The mRNA expression and relationships with overall survival duration for the ovarian cancer patients were analyzed using GraphPad Prism 8.0 software.

Statistical Analysis

Data were analyzed by Student's *t*-test using GraphPad Prism 8.0 software. *P* values < 0.05 were considered statistically significant.

Results

S1PR1 overexpression affects acquired resistance to chemotherapies in ovarian carcinoma by upregulating P-STAT3.

We found that S1PR1 expression correlated with poor survival rates in ovarian cancer patients by analyzing the TCGA database (Figure 1A). In addition previous studies confirmed that S1PR1 enhances ovarian cancer progression¹⁹ and assists chemotherapy resistance in tumors,¹³ which suggests that S1PR1 acts as an oncogene in ovarian carcinoma and may be associated with chemoresistance in ovarian cancer. Given that DDP is the most widely used chemotherapy in ovarian cancer treatment and that there is no better model for resistance to the agent, we transformed SKOV3 ovarian cancer cells into cisplatin-resistant SKOV3DR cells by exposing them to escalating doses of DDP for 2 months. Figure 1B shows data confirming the successful generation of a DDP-resistant ovarian cancer cell line from the parental cells (resistance index for DDP: 5). In addition, the ABC family gene multidrug resistance protein 1 (MDR1), as a marker of drug efflux was evaluated to further confirm drug resistance in the DDP-resistant preclinical model (Figure 1C). We also tested the expression of S1PR1 as well as the phosphorylation of its downstream signaling molecule STAT3 in SKOV3DP and SKOV3DR cells at the protein level. Figure 1C shows that the S1PR1 and P-STAT3 levels were elevated in SKOV3DR cells. In addition, Zhang et al analyzed the original TCGA ovarian cancer data and found that the P-STAT3 level was greatly enhanced in patients with shorter survival compared with those with longer survival,⁹ in accordance with the results of researchers who found that P-STAT3 was elevated in ovarian cancer to facilitate survival and promote drug resistance.^{10,11} To confirm the role of S1PR1 in drug resistance, S1PR1 was silenced in SKOV3DR cells by two different siRNAs (si1 and si2), and the changes in the mRNA and protein levels of S1PR1 were evaluated by qPCR and Western blot assays (Figure 1D and E). In addition, the protein levels of P-STAT3 were decreased in SKOV3DR cells expressing S1PR1 siRNA (Figure 1E), suggesting that the level of phosphorylation of STAT3 is positively associated with S1PR1 expression. MTT assays showed that knocking down S1PR1 led to a significant reversal of DDP resistance in SKOV3DR cells compared to administering the nontargeting siRNA control (Figure 1F).

BAF312 downregulates S1PR1, inhibits STAT3 activity and promotes the apoptosis of SKOV3DR cells to resensitize DDP-resistant ovarian cancer cells.

We examined the effects of BAF312 (Figure 2A), a small-molecule selective antagonist of S1PR1, on SKOV3DR cells. Cells were pretreated with BAF312 at the indicated concentrations for 72 h and then incubated with MTT. Figure 2B

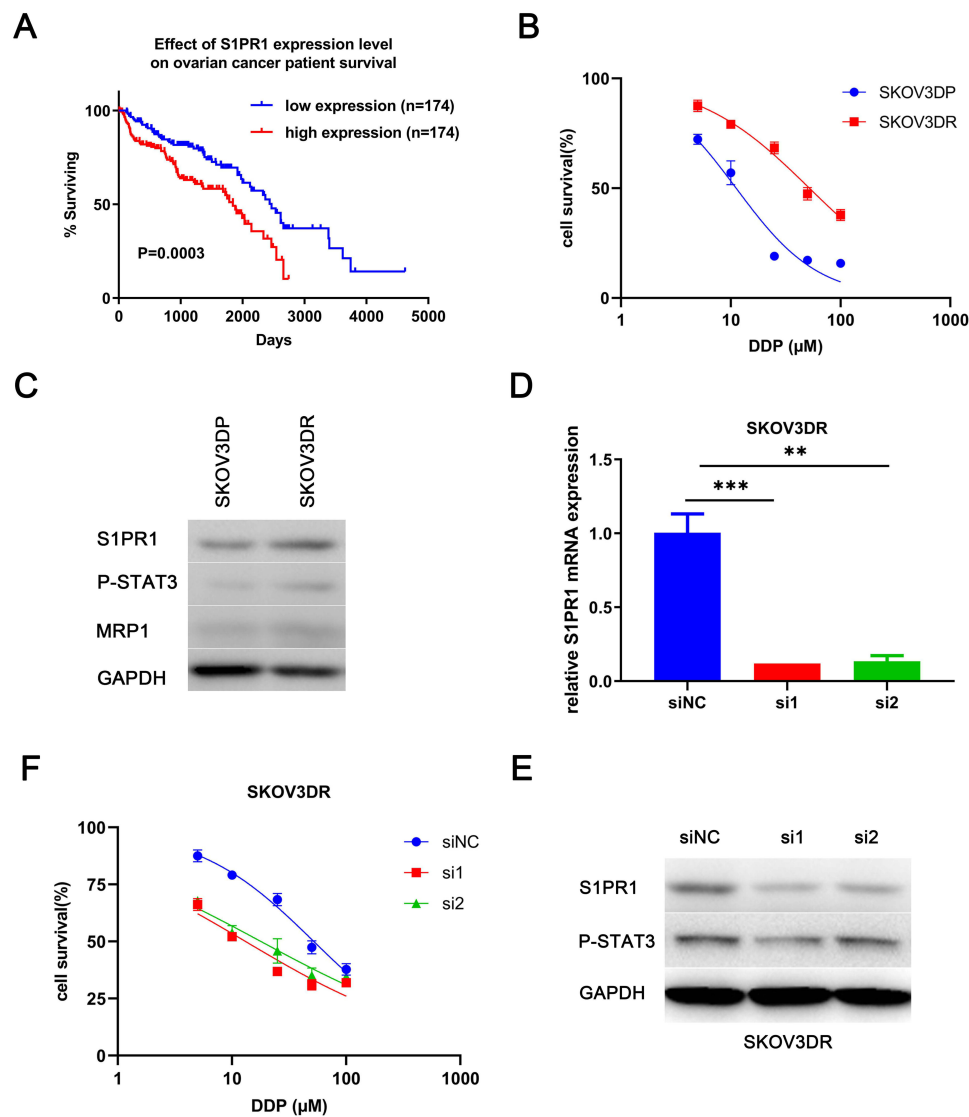


Figure 1 S1PR1 is highly expressed in the DDP-resistant ovarian cancer cell line SKOV3DR and has a positive relationship with P-STAT3. **Notes:** (A) TCGA database analysis of the relationship between S1PR1 expression and ovarian cancer patient survival. (B) MTT assay analysis of the viability of established ovarian cancer cell lines after treatment with DDP for 3 days. (C) Western blot analysis of the protein levels of S1PR1, P-STAT3, and MRP1 in SKOV3DP parental cells and SKOV3DR DDP-resistant ovarian cancer cells. (D) qPCR analysis of S1PR1 expression in SKOV3DR-siRNA cells. Mean \pm SEM, $n = 3$, $^{**}P < 0.01$, $^{***}P < 0.001$. (E) Western blot analysis of the protein levels of S1PR1 and P-STAT3 in SKOV3DR-siRNA cells. (F) MTT assay analysis of the viability of SKOV3DR-siRNA cells treated with DDP for 72 h.

shows that BAF312 effectively decreased SKOV3DR cell viability, and the half maximal inhibitory concentration (IC₅₀) in SKOV3DR cells was 13.91 μ M. Furthermore, BAF312 (at 10 μ M) decreased the levels of S1PR1 and P-STAT3 in SKOV3DR cells (Figure 2C and D). We treated SKOV3DR-siS1PR1 cells with BAF312 and found that BAF312 barely inhibited the viability of SKOV3DR-siS1PR1 cells compared to that seen in cells administered the nontargeting siRNA control (Figure 2E), which further suggests that BAF312 selectively inhibits the viability of SKOV3DR cells by targeting S1PR1. Since downregulation

of S1PR1 by BAF312 inhibits STAT3 activation, as STAT3 activation had previously been demonstrated to be associated with chemoresistance^{10,11} and S1PR1 had been found to be upregulated in cisplatin-resistant SKOV3DR cells, we next assessed whether BAF312 could restore sensitivity to cisplatin in SKOV3DR cells. We selected a concentration of cisplatin (5 μ M) that did not alter cell growth in SKOV3DR cells after 72 h (Figure 2F) to assess the BAF312 (5 μ M) effect. Apoptosis assays confirmed that BAF312 sensitized SKOV3DR cells to cisplatin (Figure 2G and H). These results suggest that BAF312 effectively inhibits the viability of

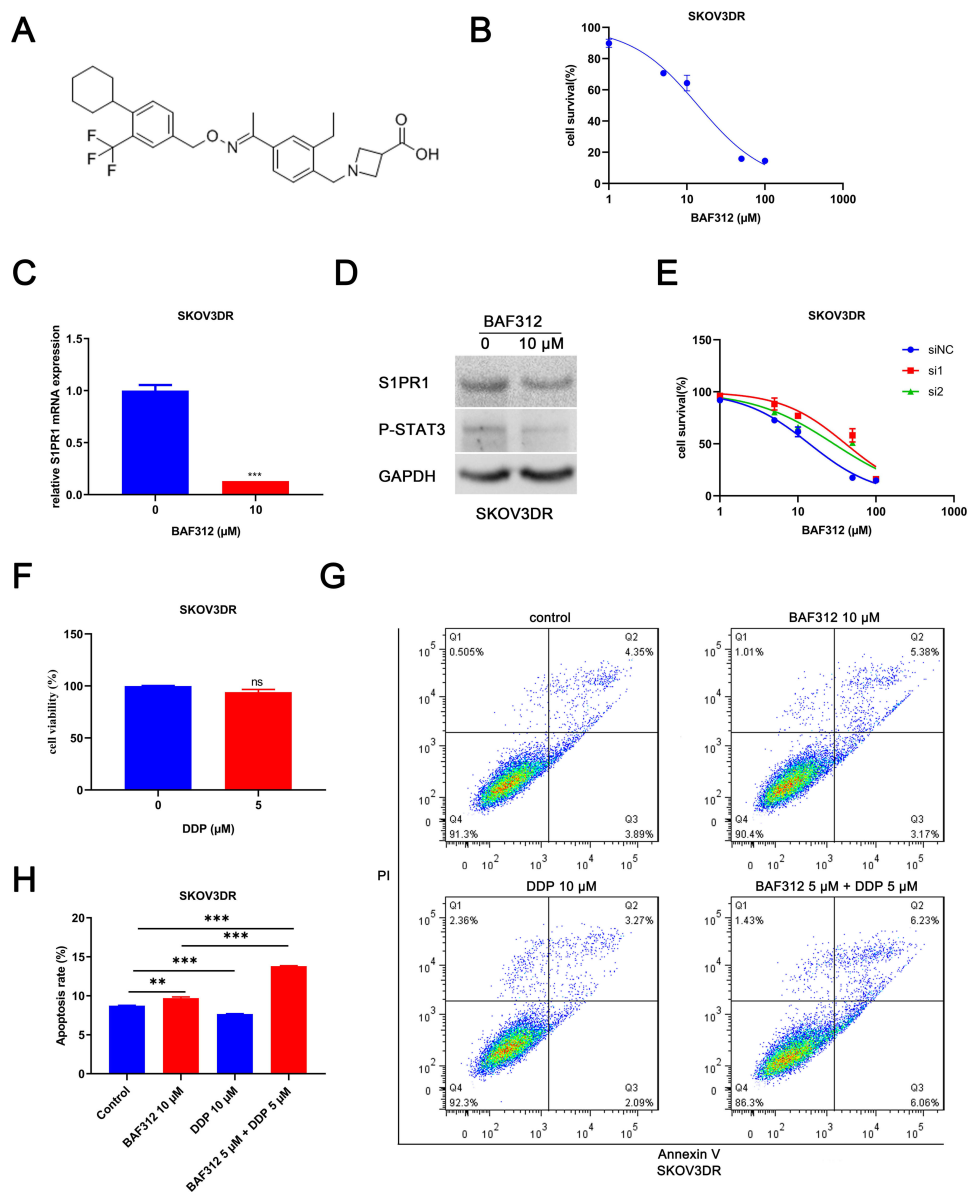


Figure 2 BAF312 decreases SIP1R and P-STAT3 levels and promotes apoptosis in SKOV3DR cells. **Notes:** (A) The chemical structure of BAF312. (B) MTT assay analysis of the viability of SKOV3DR cell lines after treatment with BAF312 for 72 h. (C) qPCR analysis of SIP1R expression in SKOV3DR cells following treatment with 10 μ M BAF312 for 2 days. Mean \pm SEM, n = 3, ***P < 0.001. (D) Western blot analysis of the protein levels of SIP1R and P-STAT3 in SKOV3DR cells following treatment with 10 μ M BAF312 for 2 days. (E) MTT assay analysis of the viability of SKOV3DR-siRNA cells treated with BAF312 for 72 h. (F) MTT assay analysis of the viability of SKOV3DR cells treated with the indicated concentrations of DDP for 72 h. Mean \pm SEM, n=5, ns P>0.05. (G) Apoptosis assay analysis of the apoptotic ratio of SKOV3DR cell lines after incubation with 10 μ M BAF312, 10 μ M DDP, and 5 μ M BAF312 + 5 μ M DDP for 2 days. (H) The statistical results of the apoptotic ratio for SKOV3DR cells. Mean \pm SEM, n = 3, **P < 0.01, ***P < 0.001.

SKOV3DR cells by downregulating SIP1R and P-STAT3 and restores sensitivity to DDP in SKOV3DR cells.

Shell-Core Nanoparticles encapsulate BAF312.

BAF312-DSPE-PEG2000-COOH-CaP nanoparticles (BAF312@CaP-NPs) were synthesized via a repeatable biomineralization method in which hydrophobic DSPE encapsulating BAF312 formed the compact inner core and hydrophilic PEG2000 with calcium phosphate (CaP) formed the outer shell (Figure 3A). TEM results showed that

BAF312@CaP-NPs with the shell-core structure had a spherical appearance and were homogeneously dispersed in aqueous solution (Figure 3B). The diameter of the BAF312@CaP-NPs was 116 ± 4.341 nm with a PDI of 0.225 ± 0.009 in aqueous solution (Figure 3B). The stability of BAF312@CaP-NPs was evaluated by measuring the size of the NPs following incubation at 37°C in 5% serum solution (pH 7.4). The size and PDI of NPs showed nearly no change for seven days, suggesting the stability of NPs in the

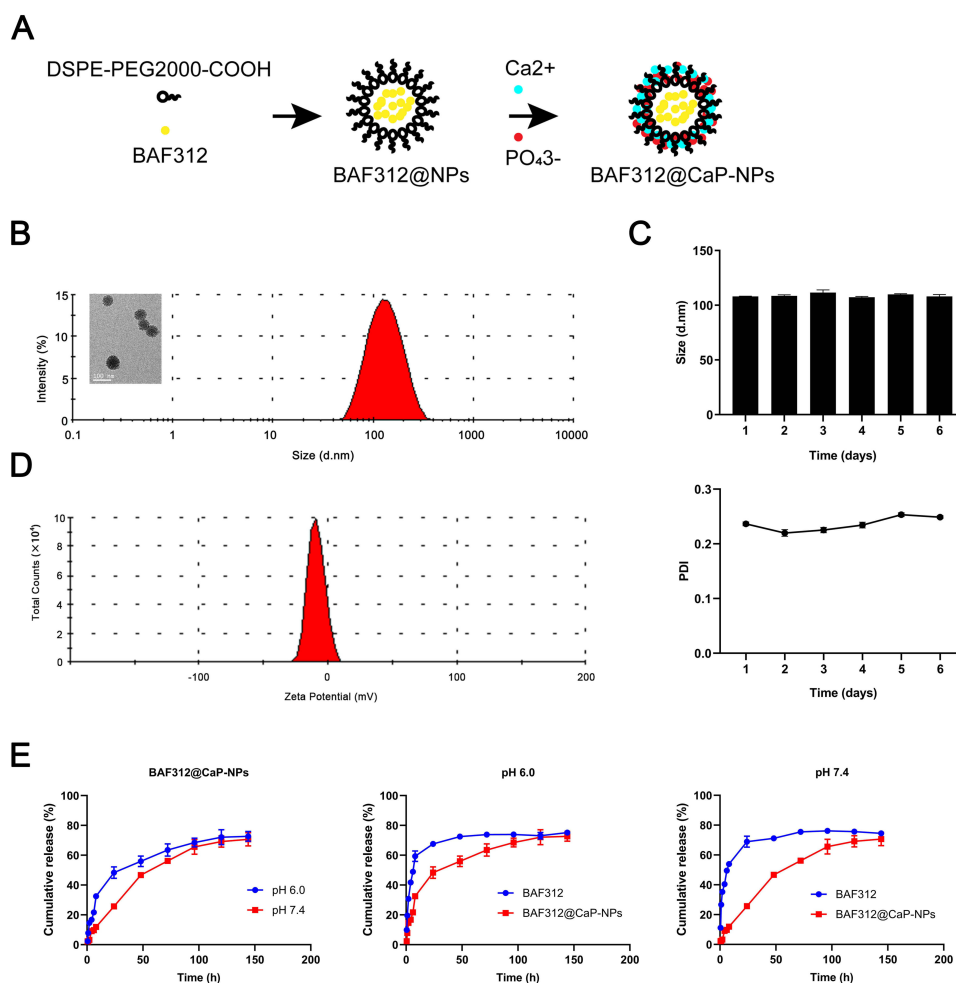


Figure 3 The formation and characterization of shell-core BAF312@CaP-NPs. **Notes:** (A) The BAF312@CaP-NPs were prepared by the biomimetic method in which an organic DSPE-PEG2000 core encapsulates BAF312 followed by adsorption of CaP to the inorganic porous shell. (B) TEM showed BAF312@CaP-NPs with a shell-core spherical structure. The hydrodynamic size of BAF312@CaP-NPs was 116 ± 4.341 nm, with a PDI of 0.225 ± 0.009 . (C) The average potential of BAF312@CaP-NPs in aqueous solution (pH 7.4) was -9.67 ± 0.935 mV. (D) The size and PDI of BAF312@CaP-NPs were evaluated for 6 days. (E) HPLC analysis of the release profiles of free-BAF312 and BAF312 from NPs at pH 6.0 and 7.4.

blood circulation (Figure 3C). In aqueous solution (pH 7.4), BAF312@CaP-NPs were negatively charged with a zeta potential of -9.67 ± 0.935 mV (Figure 3D). However, in the aqueous solution of pH 6.0, the NPs were slightly positively charged with a zeta potential of $+12.5 \pm 0.006$ mV (Figure S1). In addition, the drug loading (DL%) value was 12.68% for BAF312, and the encapsulation efficiency (EE%) value was 76.1% for BAF312, which suggests that it has few side effects and high therapeutic functions. The CaP serves as a pH sensor and enhanced the release of BAF312 in the acidic environment. The dialysis assay showed that BAF312 was released more quickly in a solution of pH 6.0 than in a solution of pH 7.4 (Figure 3E).

Nanoparticles enhance cellular uptake and greatly promote apoptosis by downregulating S1PR1 and inhibiting STAT3 activation.

A prerequisite for an antitumor effect is that tumor cells can effectively internalize the drug. In this section, we follow the process of transporting core-shell nanoparticles into ovarian cancer cells via a fluorescence microscopy assay. BAF312 was replaced with the fluorescent dye Rb to create Rb@CaP-NPs, which could be used to track NPs in ovarian cancer cells. Under an inverted fluorescence microscope, the fluorescence intensities were observed as follows: free Rb group < Rb@CaP-NPs, indicating that NPs improve the internalization of the drugs (Figure 4A). The effects of BAF312@CaP-NPs were assessed using apoptosis experiments. In this study, the apoptotic rate of cisplatin-resistant SKOV3DR ovarian cancer cells was observed in the following order: control < CaP-NPs < BAF312 < BAF312@CaP-NPs (Figure 4B and C). Calcium indicator and PI staining analysis of apoptosis also indicated that BAF312@CaP-NPs

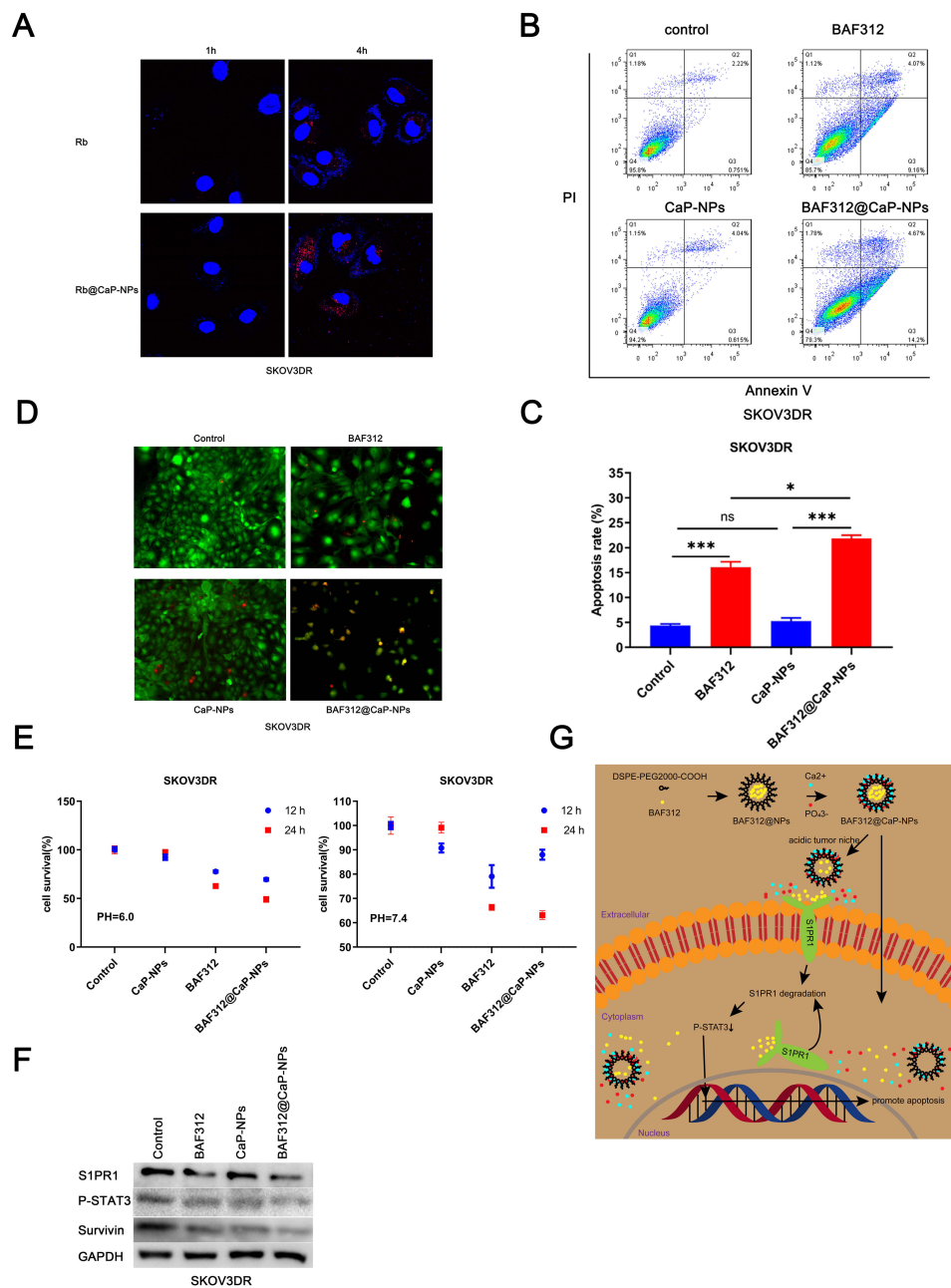


Figure 4 BAF312@CaP-NPs dramatically boost the apoptosis of SKOV3DR cells by inhibiting S1PR1 and downregulating P-STAT3. **Notes:** (A) Fluorescence microscopy analysis of the cellular uptake of tumor-targeted shell-core nanoparticles in SKOV3DR cell lines. (B) Apoptosis assay analysis of the apoptotic ratio of SKOV3DR cell lines after incubation with 10 μ M BAF312, 10 μ M BAF312@CaP-NPs and an equal amount of control CaP-NPs for 2 days. (C) The statistical results of the apoptotic ratio for SKOV3DR cells. Mean \pm SEM, n = 3, ns P > 0.05, *P < 0.05, ***P < 0.001. (D) Calcium indicator and PI staining analysis of apoptosis in SKOV3DR cells following incubation with 10 μ M BAF312, 10 μ M BAF312@CaP-NPs and an equal amount of control CaP-NPs for 3 days. The red represents PI positivity, the green represents calcium positivity, and the yellow represents both PI and calcium positivity. (E) MTT assay analysis of the viability of SKOV3DR cells treated with BAF312 for 12 h and 24 h in pH 6.0 and pH 7.4 medium, respectively. (F) Western blot analysis of the protein levels of S1PR1, P-STAT3, and survivin in SKOV3DR cells following treatment with 10 μ M BAF312, 10 μ M BAF312@CaP-NPs and an equal amount of control CaP-NPs for 2 days. (G) Schematic diagram of BAF312@CaP-NPs killing ovarian cancer cells.

effectively promoted the apoptosis of SKOV3DR cells (Figure 4D). The MTT assay was used to test the viability of SKOV3DR cells incubated with certain kinds of drugs for 12 h and 24 h in tumor niches of two different pH values (6.0 and 7.4). Figure 4E shows that NPs in the acidic niche tended

to rapidly and significantly decrease the viabilities of SKOV3DR cells. The results suggested that BAF312@CaP-NPs greatly enhanced the cytotoxicity of BAF312 in the cisplatin-resistant ovarian carcinoma cell line SKOV3DR. Compared with BAF312 alone, BAF312@CaP-NPs showed

a better ability to induce SKOV3DR cell apoptosis, which indicates the advantages of NPs in terms of pH sensitivity, modifiable voltage in the acidic tumor niche,²⁶ and appropriate size, which were beneficial for passive tumor targeting through the enhanced permeability and retention (EPR) effect.²⁴ As shown in Figure 4F, the levels of S1PR1, P-STAT3 and the anti-apoptosis protein survivin were evaluated by Western blotting. BAF312@CaP-NPs effectively inhibited S1PR1 and P-STAT3 and downregulated the expression of the apoptosis inhibitor survivin. These results confirm that BAF312@CaP-NPs indeed promote the apoptosis of cisplatin-resistant ovarian cancer cells by inhibiting S1PR1 and downregulating the phosphorylation of STAT3 protein. Figure 4G shows a schematic diagram of BAF312@CaP-NPs killing ovarian cancer cells.

Discussion

Most ovarian cancer patients are sensitive to platinum- or taxane-based therapies; however, they subsequently tend to develop acquired drug resistance.^{1,4,5} Chemoresistance remains a barrier in the treatment of ovarian cancer.

Early studies have demonstrated aberrant activity of STAT3 in ovarian cancers.⁶ Moreover, studies have elucidated that activated STAT3 levels are higher in ovarian tumors than in adjacent normal ovarian tissue.⁹ In addition, previous studies found that relatively high intracellular activated STAT3 levels induced chemoresistance.^{10,27} However, there is no available inhibitor for activated STAT3 in the clinic. Hence, targeting the activator of STAT3 could be a potent replacement. S1PR1 was found to be an activator of STAT3 in ovarian cancer cells.¹⁹ In addition, S1PR1 was also found to be overexpressed in ovarian cancer tissues compared with normal ovarian tissues.^{28,29} Taken together, these studies indicate that S1PR1 is a novel therapeutic target for ovarian cancer.

In this study, we found that S1PR1 was overexpressed in SKOV3DR cells but not in SKOV3DP cells. Combined with previous studies that confirmed that targeting S1PR1 in ovarian cancer induces apoptosis, decreases cell viability, and reverses cisplatin resistance by inhibiting the activity of STAT3,^{13,15,19} these results suggest that S1PR1 could be a potent target for downregulating P-STAT3 and promoting apoptosis. The overexpression of S1PR1 in cisplatin-resistant ovarian cancer cells makes it an attractive target for neoadjuvant chemotherapy and shows its potential to be an independent target for deciphering the different contributions of cells in the tumor niche. Our work showed that

downregulating S1PR1 in cisplatin-resistant ovarian cancer cells increased the sensitivity to cisplatin.

Many studies have demonstrated that S1PR1 increases activated STAT3 levels via different mechanisms and would be predicted to have additive or synergistic effects.^{13–15} In addition, some works have proven that downregulating S1PR1 elicits anticancer activity by disrupting signaling pathways that regulate cell proliferation, angiogenesis and motility.^{30–32} Our work found that the sphingosine analogue BAF312, a selective inhibitor of S1PR1, could effectively decrease intracellular levels of activated STAT3 by decreasing S1PR1 and enhancing apoptosis and could be applied to effectively treat cisplatin-resistant ovarian cancer by downregulating S1PR1 and inhibiting STAT3 activity. These observations suggest that therapeutic regulation of sphingolipid metabolism to decrease activated STAT3 levels might be an effective approach for the treatment of ovarian tumors, and the data in this study are in accordance with this hypothesis. In vitro data demonstrate that BAF312 enhances the cytotoxicity of cisplatin in ovarian cancer cell lines with a known pattern of resistance to cisplatin. In addition, our work found that BAF312 + cisplatin exerts synergistic antiproliferative effects in vitro. This is the first preclinical evaluation of the efficacy of BAF312 + cisplatin in ovarian cancer.

Specifically, with reference to ovarian cancer, in vitro BAF312 cytotoxicity is independent of sensitivity to cisplatin. We proposed that BAF312 might be effectively combined with cisplatin to overcome resistance to more conventional agents.

In our study, we discovered that downregulation of S1PR1 using siRNA resulted in increased cisplatin sensitivity in cisplatin-resistant SKOV3DR cells in vitro. Our study, for the first time, demonstrates that targeting S1PR1 inhibits ovarian cancer cell viability and enhances the cisplatin sensitivity of cisplatin-resistant SKOV3DR cells. Because BAF312 selectively targets S1PR1 but not S1PR2, S1PR3, or S1PR4,¹⁶ we chose BAF312 to treat the cisplatin-resistant ovarian cancer cell line SKOV3DR. The results reveal that BAF312 diminishes the viability of cisplatin-resistant ovarian cancer cells at low drug concentrations. While the insoluble property of BAF312 limits its usage in ovarian cancer, we designed a drug delivery system by packaging BAF312 into nanoparticles with a PEG hydrophilic chain and degradable CaP (calcium ions and phosphate ions) shell with smart pH sensitivity (BAF312@CaP-NPs). The negative charge and proper size of the shell-core structure of BAF312@CaP-NPs ensure long-term circulation and effective penetration

through the discontinuous tumor vasculature via EPR effects. In addition, the acidic niche of the tumor enabled the NPs to turn into positively charged NPs, which enhanced the uptake of NPs by tumor cells.^{25,26} These nanoparticles are biocompatible, have low toxicity, are biodegradable, and have low immunogenicity. In addition, using the nanoparticle packaging system avoids the dose-limiting toxicities inherent to drugs that travel through the blood.

Current treatment for ovarian cancer patients leads to a high initial response rate, but most patients develop progressive resistance to disease within a few months of diagnosis.^{33–37} Therefore, there is an urgent need for alternative drugs to treat drug-resistant ovarian tumors. Our works suggest that novel nanoparticles BAF312@CaP-NPs deserve further evaluation for the treatment of this tumor type.

Conclusion

Our work found that S1PR1 affected acquired chemoresistance in ovarian cancer by increasing the P-STAT3 level. Further, we found that BAF312@CaP-NPs selectively targeted S1PR1 and greatly reduced the viability of S1PR1-mediated cisplatin-resistant ovarian cancer cells by inhibiting P-STAT3. We suggest that BAF312@CaP-NPs deserve further evaluation for the treatment of chemoresistance tumor type.

Abbreviations

S1PR1, sphingosine-1-phosphate receptor-1; P-STAT3, phosphorylated-signal transduction and activators of transcription 3; BAF312, siponimod; DDP, cisplatin; FDA, Food and Drug Administration; DSPE-PEG2000-COOH, 1,2-distearoyl-sn-glycero-3-phosphoethanolamine-N-[carboxy(polyethylene glycol)-2000]; MRP1, multidrug resistance-associated protein 1; FITC, fluorescein isothiocyanate; MTT, 3-(4,5-dimethylthiazol-2-yl)-2,5-diphenyltetrazolium bromide; PI, propidium iodide; PDI, polydispersity index; TEM, transmission electron microscopy; HPLC, high-performance liquid chromatography; EE, encapsulation efficiencies; LE, loading efficiency; DMSO, dimethyl sulfoxide.

Acknowledgments

This research was supported by the National Natural Science Foundation of China (No. 81972886, No. 81773272, No. 81771839, No. 81671687 and No. 81874479), the State Key Laboratory of Oncogenes and Related Genes (No. 91-17-20), Medical-Engineering Joint Funds from Shanghai Jiao Tong University (No. YG2017QN43), Shanghai

Municipal Commission of Health and Family Planning (No. 20174Y0123).

Disclosure

The authors report no conflicts of interest in this work.

References

- Clamp AR, James EC, McNeish IA, et al. Weekly dose-dense chemotherapy in first-line epithelial ovarian, fallopian tube, or primary peritoneal carcinoma treatment (ICON8): primary progression free survival analysis results from a GCIg phase 3 randomised controlled trial. *Lancet*. 2019;394(10214):2084–2095. doi:10.1016/S0140-6736(19)32259-7
- Dai Y, Ma P, Cheng Z, et al. Up-conversion cell imaging and pH-induced thermally controlled drug release from NaYF₄/Yb₃+Er₃+@hydrogel core-shell hybrid microspheres. *ACS Nano*. 2012;6(4):3327–3338. doi:10.1021/nm300303q
- Huang Z, Zhou W, Li Y, et al. Novel hybrid molecule overcomes the limited response of solid tumours to HDAC inhibitors via suppressing JAK1-STAT3-BCL2 signalling. *Theranostics*. 2018;8(18):4995–5011. doi:10.7150/thno.26627
- Wojtaszek JL, Chatterjee N, Najeeb J, et al. A small molecule targeting mutagenic translesion synthesis improves chemotherapy. *Cell*. 2019;178(1):152–159. doi:10.1016/j.cell.2019.05.028
- Jayson GC, Kohn EC, Kitchener HC, Ledermann JA. Ovarian cancer. *Lancet*. 2014;384(9951):1376–1388. doi:10.1016/S0140-6736(13)62146-7
- Permeth-Wey J, Fulp WJ, Reid BM, et al. STAT3 polymorphisms may predict an unfavorable response to first-line platinum-based therapy for women with advanced serous epithelial ovarian cancer. *Int J Cancer*. 2016;138(3):612–619. doi:10.1002/ijc.29799
- Jung JG, Shih IM, Park JT, et al. Ovarian cancer chemoresistance relies on the stem cell reprogramming factor PBX1. *Cancer Res*. 2016;76(21):6351–6361. doi:10.1158/0008-5472.CAN-16-0980
- Shu T, Li Y, Wu X, Li B, Liu Z. Down-regulation of HECTD3 by HER2 inhibition makes serous ovarian cancer cells sensitive to platinum treatment. *Cancer Lett*. 2017;411:65–73. doi:10.1016/j.canlet.2017.09.048
- Zhang H, Liu T, Zhang Z, et al. Integrated proteogenomic characterization of human high-grade serous ovarian cancer. *Cell*. 2016;166(3):755–765. doi:10.1016/j.cell.2016.05.069
- Yue P, Zhang X, Paladino D, et al. Hyperactive EGF receptor, Jaks and Stat3 signaling promote enhanced colony-forming ability, motility and migration of cisplatin-resistant ovarian cancer cells. *Oncogene*. 2012;31(18):2309–2322. doi:10.1038/onc.2011.409
- Bixel K, Saini U, Kumar BH, et al. Targeting STAT3 by HO3867 induces apoptosis in ovarian clear cell carcinoma. *Int J Cancer*. 2017;141(9):1856–1866. doi:10.1002/ijc.30847
- Levina V, Nolen BM, Marrangoni AM, et al. Role of eotaxin-1 signaling in ovarian cancer. *Clin Cancer Res*. 2009;15(8):2647–2656. doi:10.1158/1078-0432.CCR-08-2024
- Lee H, Deng J, Kujawski M, et al. STAT3-induced S1PR1 expression is crucial for persistent STAT3 activation in tumors. *Nat Med*. 2010;16(12):1421–1428. doi:10.1038/nm.2250
- Liu Y, Deng J, Wang L, et al. S1PR1 is an effective target to block STAT3 signaling in activated B cell-like diffuse large B-cell lymphoma. *Blood*. 2012;120(7):1458–1465. doi:10.1182/blood-2011-12-399030
- Liang J, Nagahashi M, Kim EY, et al. Sphingosine-1-phosphate links persistent STAT3 activation, chronic intestinal inflammation, and development of colitis-associated cancer. *Cancer Cell*. 2013;23(1):107–120. doi:10.1016/j.ccr.2012.11.013

16. Al-Salama ZT. Siponimod: first global approval. *Drugs*. 2019;79(9):1009–1015. doi:10.1007/s40265-019-01140-x
17. O'Sullivan C, Schubart A, Mir AK, Dev KK. The dual S1PR1/S1PR5 drug BAF312 (Siponimod) attenuates demyelination in organotypic slice cultures. *J Neuroinflammation*. 2016;13:31. doi:10.1186/s12974-016-0494-x
18. Vogelgesang A, Domanska G, Ruhnau J, Dressel A, Kirsch M, Schulze J. Siponimod (BAF312) treatment reduces brain infiltration but not lesion volume in middle-aged mice in experimental stroke. *Stroke*. 2019;50(5):1224–1231. doi:10.1161/STROKEAHA.118.023667
19. McCann GA, Naidu S, Rath KS, et al. Targeting constitutively-activated STAT3 in hypoxic ovarian cancer, using a novel STAT3 inhibitor. *Oncoscience*. 2014;1:216–228. doi:10.18632/oncoscience.26
20. Demont EH, Arpino S, Bit RA, et al. Discovery of a brain-penetrant S1P₃-sparing direct agonist of the S1P₁ and S1P₅ receptors efficacious at low oral dose. *J Med Chem*. 2011;54(19):6724–6733. doi:10.1021/jm200609t
21. Kreitzburg KM, Fehling SC, Landen CN, et al. FTY720 enhances the anti-tumor activity of carboplatin and tamoxifen in a patient-derived xenograft model of ovarian cancer. *Cancer Lett*. 2018;436:75–86. doi:10.1016/j.canlet.2018.08.015
22. Veronese FM, Pasut G. PEGylation, successful approach to drug delivery. *Drug Discov Today*. 2005;10(21):1451–1458. doi:10.1016/S1359-6446(05)03575-0
23. Yuan H, Li X, Zhang C, et al. Nanosuspensions as delivery system for gambogic acid: characterization and in vitro/in vivo evaluation. *Drug Deliv*. 2016;23(8):2772–2779. doi:10.3109/10717544.2015.1077294
24. Kobayashi H, Watanabe R, Choyke PL. Improving conventional enhanced permeability and retention (EPR) effects; what is the appropriate target. *Theranostics*. 2013;4(1):81–89. doi:10.7150/thno.7193
25. Takemoto H, Miyata K, Hattori S, et al. Acidic pH-responsive siRNA conjugate for reversible carrier stability and accelerated endosomal escape with reduced IFN α -associated immune response. *Angew Chem Int Ed Engl*. 2013;52(24):6218–6221. doi:10.1002/anie.201300178
26. Zhou Z, Shen Y, Tang J, et al. Charge-reversal drug conjugate for targeted cancer cell nuclear drug delivery. *Adv Funct Mater*. 2009;19(22):3580–3589. doi:10.1002/adfm.200900825
27. Dijkgraaf EM, Heusinkveld M, Tummers B, et al. Chemotherapy alters monocyte differentiation to favor generation of cancer-supporting M2 macrophages in the tumor microenvironment. *Cancer Res*. 2013;73(8):2480–2492. doi:10.1158/0008-5472.CAN-12-3542
28. Ahn JH, Kim TJ, Lee JH, Choi JH. Mutant p53 stimulates cell invasion through an interaction with Rad21 in human ovarian cancer cells. *Sci Rep*. 2017;7(1):9076. doi:10.1038/s41598-017-08880-4
29. Wen Z, Zhao S, Liu S, Liu Y, Li X, Li S. MicroRNA-148a inhibits migration and invasion of ovarian cancer cells via targeting sphingosine-1-phosphate receptor 1. *Mol Med Rep*. 2015;12(3):3775–3780. doi:10.3892/mmr.2015.3827
30. Lankadasari MB, Aparna JS, Mohammed S, et al. Targeting S1PR1/STAT3 loop abrogates desmoplasia and chemosensitizes pancreatic cancer to gemcitabine. *Theranostics*. 2018;8(14):3824–3840. doi:10.7150/thno.25308
31. Balaji RVA, Anwar M, Akhter MZ, et al. Sphingosine-1-phosphate receptor 1 activity promotes tumor growth by amplifying VEGF-VEGFR2 angiogenic signaling. *Cell Rep*. 2019;29(11):3472–3487. doi:10.1016/j.celrep.2019.11.036
32. Li C, Zheng S, You H, et al. Sphingosine 1-phosphate (S1P)/S1P receptors are involved in human liver fibrosis by action on hepatic myofibroblasts motility. *J Hepatol*. 2011;54(6):1205–1213. doi:10.1016/j.jhep.2010.08.028
33. Yang D, Khan S, Sun Y, et al. Association of BRCA1 and BRCA2 mutations with survival, chemotherapy sensitivity, and gene mutator phenotype in patients with ovarian cancer. *JAMA*. 2011;306(14):1557–1565. doi:10.1001/jama.2011.1456
34. Swisher EM, Lin KK, Oza AM, et al. Rucaparib in relapsed, platinum-sensitive high-grade ovarian carcinoma (ARIEL2 Part 1): an international, multicentre, open-label, phase 2 trial. *Lancet Oncol*. 2017;18(1):75–87. doi:10.1016/S1470-2045(16)30559-9
35. Kang X, Yu Y, Chen Z, et al. A negatively charged Pt(IV) prodrug for electrostatic complexation with polymers to overcome cisplatin resistance. *J Mater Chem B*. 2019;7(21):3346–3350. doi:10.1039/C9TB00155G
36. Zhao MD, Li JQ, Chen FY, et al. Co-delivery of curcumin and paclitaxel by “core-shell” targeting amphiphilic copolymer to reverse resistance in the treatment of ovarian cancer. *Int J Nanomedicine*. 2019;14:9453–9467. doi:10.2147/IJN.S224579
37. Stilgenbauer M, Jayawardhana AM, Datta P, et al. A spermine-conjugated lipophilic Pt(IV) prodrug designed to eliminate cancer stem cells in ovarian cancer. *Chem Commun (Camb)*. 2019;55(43):6106–6109. doi:10.1039/C9CC02081K

International Journal of Nanomedicine

Publish your work in this journal

The International Journal of Nanomedicine is an international, peer-reviewed journal focusing on the application of nanotechnology in diagnostics, therapeutics, and drug delivery systems throughout the biomedical field. This journal is indexed on PubMed Central, MedLine, CAS, SciSearch®, Current Contents®/Clinical Medicine,

Submit your manuscript here: <https://www.dovepress.com/international-journal-of-nanomedicine-journal>

Dovepress

Journal Citation Reports/Science Edition, EMBASE, Scopus and the Elsevier Bibliographic databases. The manuscript management system is completely online and includes a very quick and fair peer-review system, which is all easy to use. Visit <http://www.dovepress.com/testimonials.php> to read real quotes from published authors.